THE JOURNAL OF BIOLOGICAL CHEMISTRY VOL. 283, NO. 3, pp. 1492–1500, January 18, 2008

The Rac1 Polybasic Region Is Required for Interaction with Its Effector PRK1*◆

Received for publication, August 14, 2007, and in revised form, October 25, 2007 Published, JBC Papers in Press, November 15, 2007, DOI 10.1074/jbc.M706760200

Rakhee Modha, Louise J. Campbell, Daniel Nietlispach, Heeran R. Buhecha, Darerca Owen[1], and Helen R. Mott[2]

From the Department of Biochemistry, University of Cambridge, 80, Tennis Court Road, Cambridge CB2 1GA, United Kingdom

Protein kinase C-related kinase 1 (PRK1 or PKN) is involved in regulation of the intermediate filaments of the actin cytoskeleton, as well as having effects on processes as diverse as mitotic timing and apoptosis. It is activated by interacting with the Rho family small G proteins and arachidonic acid or by caspase cleavage. We have previously shown that the HR1b of PRK1 binds exclusively to Rac1, whereas the HR1a domain binds to both Rac1 and RhoA. Here, we have determined the solution structure of the HR1b-Rac complex. We show that HR1b binds to the C-terminal end of the effector loop and switch 2 of Rac1. Comparison with the HR1a-RhoA structure shows that this part of the Rac1-HR1b interaction is homologous to one of the contact sites that HR1a makes with RhoA. The Rac1 used in this study included the C-terminal polybasic region, which is frequently omitted from structural studies, as well as the core G domain. The Rac1 C-terminal region reverses in direction to interact with residues in switch 2, and the polybasic region itself interacts with residues in HR1b. The interactions with HR1b do not prevent the polybasic region being available to contact the negatively charged membrane phospholipids, which is considered to be its primary role. This is the first structural demonstration that the C terminus of a G protein forms a novel recognition element for effector binding.

The small G proteins of the Ras superfamily behave as molecular switches in signal transduction, being switched on in the GTP-bound form and switched off in the GDP-bound form. They respond to extracellular stimuli through the action of guanine nucleotide exchange factors, which allow exchange of GDP for GTP. In the GTP-bound state, they can bind to downstream effector proteins, which mediate activation of their signaling pathways. They are switched off again when their intrinsic GTPase activity is stimulated by the GTPase-activating proteins (GAPs).[3] The Rho family of small G proteins, of which the best studied include RhoA, Rac1, and Cdc42, are involved in regulating a wide variety of processes, including cell growth and differentiation, cell adhesion, and cell motility (1). Many of the processes affected by the Rho family are involved in tumorigenesis and metastasis. Not surprisingly, therefore, many Rho proteins and their guanine nucleotide exchange factors are potent oncogenes.

An enormous number of effectors have been identified for the Rho family GTPases. Several of these effectors are protein kinases, and many of them appear to be regulated such that they are inhibited by intramolecular interactions in the unstimulated state. Binding of the activated, Rho family G protein leads to the release of the kinase from its inhibition, allowing it to be phosphorylated in the activation loop and thus rendering it efficacious toward its downstream targets (2).

The Ser/Thr kinases PRK1 (also known as PKN1 or PKNα), PRK2 (PKN2), and PKN3 (PKNβ) all have the same general architecture (3). They have a C-terminal kinase domain that is a member of the protein kinase C superfamily. They also contain three HR1 (for homology repeat) domains at the N terminus, HR1a-c, followed by a C2 domain that is related to the Ca^{2+}-dependent membrane-targeting domains found in protein kinase C. PRK1 was found to bind to RhoA through its HR1a repeat and, moreover, this binding activated the kinase domain (4). A potential pseudosubstrate site was found in the HR1a domain of PRK1, and a peptide encompassing this region was shown to inhibit phosphorylation by PRK1 (5). It was subsequently found that PRK1 and PRK2 could be activated by the binding of either RhoA or Rac1 (6, 7). The kinase can also be activated by caspase 3 cleavage during apoptosis (8) and binding of fatty acids such as arachidonic acid to a region between the C2 domain and the kinase domain (3).

That the PRKs play a role in a number of processes is evident from the large number of interacting proteins and phosphorylation targets that have been identified for them. Many of the proteins that bind to the PRKs are part of the cytoskeletal network. For example, PRK1 interacts with the intermediate filament proteins neurofilament and vimentin, phosphorylating them to inhibit their polymerization (3, 9). PRK1 also interacts with the actin cross-linking protein α-actinin, although there is no evidence that actinin is phosphorylated as a result (3). PRK1 has also been shown to play a role in Alzheimer disease since it

* This work was supported by Cancer Research UK Grant C11309/A5148. The costs of publication of this article were defrayed in part by the payment of page charges. This article must therefore be hereby marked "*advertisement*" in accordance with 18 U.S.C. Section 1734 solely to indicate this fact.

◆ This article was selected as a Paper of the Week.

The atomic coordinates and structure factors (code 2rmk) have been deposited in the Protein Data Bank, Research Collaboratory for Structural Bioinformatics, Rutgers University, New Brunswick, NJ (http://www.rcsb.org/).

The chemical shift assignments reported in this paper have been submitted to BioMagResBank under accession number 11010.

[1] To whom correspondence may be addressed. Tel.: 44-1223-764824; Fax: 44-1223-766002; E-mail: do@bioc.cam.ac.uk.

[2] To whom correspondence may be addressed. Tel.: 44-1223-764825; Fax: 44-1223-766002; E-mail: hrm28@bioc.cam.ac.uk.

[3] The abbreviations used are: GAP, GTPases activating protein; PBR, polybasic region; PRK, Protein kinase C-related kinase; GST, glutathione *S*-transferase; NOE, nuclear Overhauser effect; HSQC, heteronuclear single quantum correlation; NOESY, NOE spectroscopy; TOCSY, total correlation spectroscopy; TROSY, transverse relaxation-optimized spectroscopy; SPA, scintillation proximity assays; r.m.s., root mean square; r.m.s.d., r.m.s. deviation; GMPPCP, guanosine 5′-(β-methylene)triphosphate; MOPS, 4-morpholinepropanesulfonic acid.

accumulates in neurofibrillary tangles and phosphorylates the microtubule assembly protein Tau (10). Tau phosphorylation down-regulates its ability to bind to microtubules, resulting in disruption of the microtubule array *in vivo* (11). PRK1 is overexpressed in prostate cancer and binds to the androgen receptor, increasing its activity as a transcription factor, although apparently not due to phosphorylation (12). PRK1 also phosphorylates the high risk human papilloma virus E6 oncoprotein that induces degradation of the p53 tumor suppressor, suggesting that PRK1 also plays a role in virally induced cancers (13). As well as its role in cancer, PRK1 is thought to be involved in cell division. When injected into *Xenopus* embryos, it caused cleavage arrest, and it was found that PRK1 phosphorylates and inhibits Cdc24, delaying mitotic timing (14). Intriguingly, there is a body of evidence that suggests that PRK1 can localize to the nucleus; it can translocate in response to stresses such as heat shock, and it has been shown to interact with various transcription factors (15–17). Finally, the C terminus of PRK1 interacts with PDK1 (18), and PDK1 phosphorylation of PRK1/PRK2 has been shown to lead to PRK activation (19). As PDK1 is downstream of phosphatidylinositol-3 kinase, it is thought that the PDK1-PRK interaction is responsible for the effects of the insulin receptor (via phosphatidylinositol-3 kinase) on actin cytoskeleton reorganization (20).

Initially the HR1a domain of PRK1 was considered to be the only binding site for Rho family proteins, although it was later shown that the HR1b domain could also bind these GTPases (21). The role of the HR1c domain remains obscure, with no known binding partners elucidated to date. The *Drosophila melanogaster* homologue of PRK1 was shown to bind specifically to RhoA and Rac1 through distinct binding sites (7). Previously, we used scintillation proximity assays to measure the binding of RhoA and Rac1 to both the HR1a and the HR1b domains as well as the HR1ab di-domain (22). We found that RhoA binds to HR1a and HR1b but that the HR1a binding affinity was at least 5-fold higher (280 nM as opposed to >1 μM). The affinities of HR1a and HR1b for RhoA measured by fluorescence were in agreement with our results (23). Furthermore, we tested Rac1 binding to the HR1a and HR1b domains and found that it binds both of them with a high affinity ($K_d \sim 70$–170 nM).

The C terminus of small G proteins in the Ras, Rho, and Rab subfamilies is lipid-modified and provides a means of membrane attachment. Between the end of the C-terminal helix and the lipid modification site, there is a sequence that varies in both length and composition between and within the subfamilies. This hypervariable region is thought to mediate at least some of the differences between small G proteins that are otherwise closely related. Rac1 has a polybasic region (PBR) in this site, which has been shown to mediate a number of functions, including membrane attachment, nuclear localization (reviewed in Ref. 24), and binding to the exchange factor β-PIX (25). Most G protein structures and the structures of the complexes that they make with their effectors have been solved by x-ray crystallographic methods, where it was necessary to remove the flexible C termini of the G protein. Thus, information about the structures of the C-terminal regions of small G proteins is extremely limited. We found previously that the PBR at the C terminus of Rac1 was necessary for its high affinity interaction with HR1b (22) and that deletion of the PBR or mutation of any of the basic residues abrogated the binding.

Here, we describe the solution structure of the complex that HR1b makes with full-length Rac1, including the C-terminal PBR. We show that HR1b binds to Rac1 in a region that encompasses the switch regions, which change conformation on GDP/GTP exchange, but that it also contacts the C-terminal PBR of Rac1. This is the first structure of an effector complex that involves interactions with the C terminus of a small G protein. We have used the structure to model the potential complexes formed between RhoA, Rac1, and PRK1. On the basis of the available structures and mutagenesis, it likely that RhoA can bind to HR1a and HR1b simultaneously, whereas the two HR1 domains compete for binding to the same site of Rac1, Furthermore, although the PBR interacts with HR1b, several of the basic residues are still solvent-exposed and are still available to function as a secondary membrane localization signal.

MATERIALS AND METHODS

Protein Expression and Purification—The HR1b domains from PRK1 (residues 122–199) and full-length (or Δ4) Rac1 with the Q61L mutation were expressed as GST fusion proteins and purified using glutathione-agarose beads (Sigma) as described previously (22). The nucleotide bound to Rac1 was exchanged for the non-hydrolyzable analogue GMPPCP as described (26). The integrity of all proteins was determined by mass spectrometry.

Uniformly ^{15}N- and ^{13}C,^{15}N-labeled HR1b was produced by growing *Escherichia coli* BL21-CodonPlus(DE3)-RIL cells (Stratagene) harboring the expression plasmid in a medium based on MOPS buffer, supplemented with 5% labeled Celtone and $^{15}NH_4Cl$ or ^{13}C-glucose (Spectra Stable Isotopes). Uniformly ^{15}N- and ^{13}C,^{15}N-labeled Rac1 was produced in *E. coli* BL21 using the same buffer and supplements.

Uniformly ^{15}N,^{13}C,^{2}H-labeled Rac was produced as follows. *E. coli* BL21 cells were freshly transformed with the GST-Rac1 expression construct and plated on 2TY at 37 °C overnight. The cells were then streaked onto 2TY plates containing increasing amounts of ^2H_2O, in each case being incubated for 18–21 h at 37 °C before being streaked onto the next plate. The ^2H_2O levels were increased stepwise through 20, 40, 60, 80, 90, and 95%. 8 × 20 ml of 2TY in 100% ^2H_2O were inoculated with ^2H_2O-adapted cells and grown for 20 h at 37 °C. The stationary cultures were centrifuged, and the pellets were resuspended in a small volume of ^{15}N,^{13}C,^{2}H Celtone. These were used to inoculate 8 × 500 ml of filter sterilized MOPS buffer made up in 95% ^2H_2O, supplemented with 5% ^{15}N,^{13}C,^{2}H Celtone (final concentration), ^{13}C-glucose, and $^{15}NH_4Cl$. The cultures were induced at $A_{600} \sim 0.8$ by the addition of 0.1 mM isopropyl-1-thio-β-D-galactopyranoside in ^2H_2O for 5 h.

Full-length Q61L RhoA·[^{3}H]GTP was produced as described previously (22). C-terminally truncated Q61L RhoA·[^{3}H]GTP, corresponding to residues 1–186 (hereafter Δ7 RhoA) was expressed and purified in the same way as the full-length protein.

NMR Spectroscopy—NMR samples were made up in the following buffer: 10 mM Tris-HCl, pH 7.4, 200 mM NaCl, 5 mM $MgCl_2$, 10 mM dithiothreitol, 0.05% NaN_3, 10% ^2H_2O. Complex

samples were made up by mixing the two proteins in a 1:1 molar ratio and concentrating the samples to 500 μl in a Centricon-3 (Amicon). All spectra were recorded at a total protein concentration of ~0.4 mM. The following experiments were recorded (reviewed in Ref. 27 unless stated otherwise): on samples of ^{15}N- or ^{13}C,^{15}N-labeled Rac1 in complex with unlabeled HR1b, ^{15}N-HSQC, HNHA, HNCA, HN(CO)CA, CBCA(CO)NH, HNCACB, HNCO, i-HNCA (28), HN(CO)CACB, ^{13}C-HSQC, HCCH-TOCSY, ^{15}N NOESY-HSQC, ^{13}C-NOESY-HSQC, ^{13}C/^{15}N-filtered,^{13}C-separated NOESY HSQC (29); on samples of ^{15}N- or ^{13}C,^{15}N-labeled HR1b with unlabeled Rac1, ^{15}N-HSQC, ^{15}N-separated TOCSY, HN(CO)CA, HNCA, HN(CO)CACB, H(CCCO)NH, (H)CC(CO)NH, HCCH-TOCSY, ^{13}C-HSQC, ^{15}N NOESY-HSQC, ^{13}C-NOESY-HSQC, ^{13}C/^{15}N-filtered,^{13}C-separated NOESY HSQC (29); on samples of ^{15}N,^{13}C,^{2}H-labeled Rac1 with unlabeled HR1b, ^{15}N TROSY-HSQC, CT-HN(CO)CA, TROSY HNCA, TROSY HNCO, TROSY HN(CA)CO, TROSY HN(COCA)CB, TROSY HNCACB (30, 31), CC(CO)NH, ^{15}N NOESY-HSQC. The data were processed using AZARA (W. Boucher, Cambridge, UK) and analyzed using ANSIG (33). Backbone torsion angles were estimated from CA, CO, CB, N, and HA chemical shifts using the program TALOS (34). These were used as restraints for ϕ and ψ with errors of twice the standard deviation from TALOS.

Structure Calculation—Structures were calculated using CNS 1.1 (35) and ARIA 1.2 (36), where the ambiguity of the NOEs is reduced in each iteration by comparing the NOE restraints with structures from the previous iteration. The methodology was essentially as described in ref. 22, except that the high temperature dynamics was increased to 300 ps and the cooling was increased to 288 ps (144 ps cooling to 1,000 K and 144 ps cooling to 50 K).

Scintillation Proximity Assays—Affinities of RhoA proteins for GST-HR1a and GST-HR1ab were measured using scintillation proximity assays (SPAs), in which the GST fusion protein was attached to a fluoromicrosphere via an anti-GST antibody in the presence of Q63L RhoA·[^{3}H]GTP. Binding of the G protein to the GST effector brings the labeled nucleotide close enough to the scintillant to obtain a signal. Apparent K_d values were measured as described previously (26) by varying the concentration of RhoA·[^{3}H]GTP at a constant concentration of GST-HR1a or GST-HR1ab. These assays were performed with 30 nM GST fusion protein. Using this method, the upper and lower limits of the K_d values that can accurately be measured are 1 μM and 1 nM, respectively. For each affinity determination, data points were obtained for at least 10 different RhoA concentrations. Binding curves were fitted using the appropriate binding isotherms to obtain K_d values with their standard errors (26, 37).

RESULTS AND DISCUSSION

Resonance Assignments and Structure Calculation—We have previously solved the structure of the HR1b domain by NMR (22). The uncomplexed HR1b spectra and assignments from this study were used as a reference during the assignment of HR1b in the complex with Rac1. The backbone resonances were assigned using ^{15}N-separated TOCSY and NOESY experiments, aided by HNCA and HN(CO)CA triple resonance experiments and comparison of the ^{15}N-HSQC spectra recorded on the free and complexed HR1b. Side chain resonances were assigned using three-dimensional (H)C(CCO)NH, H(CCCO)NH, and HCCH-TOCSY experiments. Backbone resonance assignments were obtained for all of HR1b except residues 156–160, which reside in the hairpin between the two helices of the coiled-coil. The resonances for these residues were also absent in the free HR1b spectra. The side chains were assigned for all residues that had a backbone NH assignment, as well as for Thr-157, for which there were partial side chain assignments although no backbone resonances were visible.

As described previously, the interaction between HR1b and Rac1 requires the C-terminal polybasic region of Rac1 (22). Initial NMR experiments were recorded on both full-length Rac1 and Rac1Δ4, which had a truncation of 4 residues at the C terminus, to assess the quality of the spectra of the two proteins. It has been observed that NMR spectra of G proteins in their active form, bound to GTP or an analogue, have fewer resonances than would be expected from the sequence (38, 39). This is due to dynamics in switch 1 and switch 2, the two regions of the protein that change conformation when GTP and GDP are exchanged. Regions of proteins that are changing conformation on the millisecond time scale often disappear in NMR spectra, due to broadening of the resonances. The ^{15}N-HSQC spectrum of Rac1Δ4 had 41 fewer peaks than expected (data not shown). Some of the missing resonances will be due to loss of the switch regions, but the switches can only account for 20–25 residues. The ^{15}N-HSQC spectrum of full-length Rac1 was also missing peaks but only had 32 fewer than expected. Thus, the full-length protein was better behaved than the Rac1Δ4, and all of the spectra of the complex made with HR1b were recorded on samples containing full-length Rac1.

Full-length Rac1 was not sufficiently stable for the NMR experiments to be recorded for assignment of the free protein. In the complex with HR1b, however, the protein was stable for several weeks, and the spectra for assignment could be recorded. The HNCA and HN(CO)CA experiments recorded on the protonated sample were of a reasonable quality, but with no information about the chemical shifts of the free protein, it was not possible to assign the protein backbone on the basis of the $^{13}C\alpha$ chemical shifts alone. The large tumbling time of the complex meant that experiments that also record the Cβ shift only worked for ~30% of the residues in the protonated samples. The Cβ experiments worked well on samples containing ^{2}H,^{13}C,^{15}N-labeled Rac1 in complex with unlabeled HR1b. Most of the Rac1 backbone resonances were visible in the complex with HR1b. The backbone resonances for residues 32–41 in switch 1 were not visible in any spectra, presumably due to conformational exchange of the backbone. Subsequently side chains were assigned for most of switch I, except residues 35, 38, and 39. In contrast, most of switch 2 was visible in the backbone experiments, except residues 57, 59, 66, and 68. Again, side chains were assigned for most of these residues, except Arg-68, which was not visible in any spectra.

There were a total of 5,587 NOEs, of which 3,510 were unambiguous and 2,077 were ambiguous. These were translated by ARIA (36) into 4,686 non-duplicated restraints in the first iteration, of which 2,686 were unambiguous and 2,001 were unam-

TABLE 1
Experimental restrains and structural statistics

		<SA>[a]	<SA>$_c$[b]
No. of experimental restraints			
Unambiguous	3629		
Ambiguous	656		
Dihedral restraints	373		
Coordinate precision[c]			
r.m.s.d. of backbone atoms (Å)		0.85 ± 0.15	0.65
r.m.s.d. of heavy atoms (Å)		1.30 ± 0.14	1.17
r.m.s. deviations			
From the experimental restraints:			
NOE distances (Å)		0.023 ± 0.002	0.021
Talos dihedral angles (°)		0.774 ± 0.049	0.787
From idealized geometry:			
Bonds (Å)		0.0021 ± 0.000058	0.0020
Angles (°)		0.39 ± 0.0046	0.39
Impropers (°)		0.30 ± 0.009	0.29
Final energy			
$E_{L\text{-}J}$[d] (kJ/mol)		−2666.2 ± 9.87	−2659.18
Ramachandran analysis			
Residues in most favored regions		84.9%	87.1%
Residues in additionally allowed regions		13.1%	11.2%
Residues in generously allowed regions		1.3%	0.8%
Residues in disallowed regions		0.6%	0.8%

[a] <SA> represents the average r.m.s. deviations for the ensemble.
[b] <SA>$_c$ represents values for the structure that is closest to the mean.
[c] For residues 1–188 of Rac1 and 125–195 of HR1b.
[d] The Lennard-Jones potential was not used at any stage in the refinement.

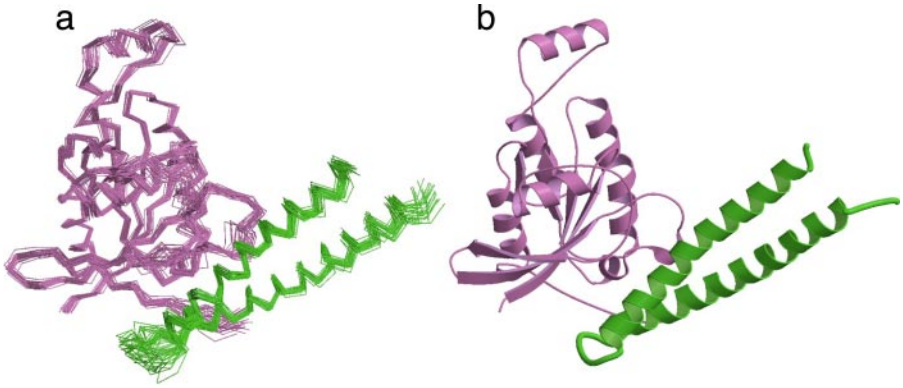

FIGURE 1. **The structure of the Rac1-HR1b complex.** In both cases, the Rac1 is colored *purple*, and the HR1b is colored *green*. All figures were produced with Molscript (49) and Raster3D (32). *a*, backbone trace of the lowest energy 25 structures. *b*, the closest structure to the mean. This structure is used in all subsequent figures.

biguous. In the final iteration, there were 3,629 unambiguous restraints and 656 ambiguous restraints. 100 structures were calculated, and of these, the 25 lowest energy structures had no NOE violation more than 0.5 Å and no dihedral violation more than 5°. The structures have good geometry and are well defined for an NMR structure of this size (Table 1), with a backbone r.m.s.d. from the mean of 0.87 Å. Free HR1b forms a coiled-coil (22), and in the complex with Rac1, it adopts essentially the same structure (Fig. 1). Rac1 forms a regular G protein fold, comprising a central six-stranded β-sheet surrounded by five α-helices, with an additional helical insert region characteristic of the Rho subfamily (40).

Interactions with the G Protein Core—HR1b contacts Rac1 at the center of the HR1b coiled-coil, whereas the N and C termini of the protein do not form any interactions with Rac1. The inter-helix loop also makes some contacts (Fig. 1). The areas of the G protein core involved in the interaction with HR1b encompass switch 1 and switch 2, the regions of the protein that are sensitive to the state of the bound nucleotide. Thus, it is likely that tight binding of HR1b to Rac1 will require the G protein to be GTP-bound. This is supported by data from other groups; Rac1 binding to PRK2 is GTP-dependent, although the binding to individual domains was not measured (6).

In Rac1, as in other G proteins, switch 2 forms an irregular α-helix. In the Rac1-HR1b complex, this helix interacts closely with both of the HR1b helices, effectively making a short section of triple coiled-coil (Figs. 1 and 2). Most of the switch 2 interactions involve residues Arg-66^{Rac1}, Leu-67^{Rac1}, and Leu-70^{Rac1}. The 2 Leu residues make extensive hydrophobic contacts with residues in both helices of HR1b: Val-141^{HR1b}, Ala-145^{HR1b}, Met-148^{HR1b}, Tyr-152^{HR1b}, Leu-162^{HR1b}, Thr-165^{HR1b}, Ala-166^{HR1b}, and Met-169^{HR1b}. The Arg-66^{Rac1} side chain forms a salt bridge with Asp-172^{HR1b} and also contacts Met-169^{HR1b} in the C-terminal helix (Figs. 2*A* and 3*A*).

HR1b also interacts with other residues in switch 2 of Rac1. The ring of Tyr-64^{Rac1} makes hydrophobic contacts with Ile-137^{HR1b}, Lys-140^{HR1b}, and Val-141^{HR1b}, whereas the Tyr-64^{Rac1} hydroxyl group contacts Lys-140^{HR1b}. Asp-63^{Rac1} is not visible in the NMR spectra, presumably because it is undergoing conformational exchange. In the structures, however, the side chain of Asp-63^{Rac1} is close to that of Gln-134^{HR1b} (Figs. 2*A* and 3*A*) and may form a hydrogen bond. Finally, Gln-74^{Rac1}, at the C terminus of switch 2, makes extensive contacts with residues in the hairpin between the HR1b helices and the start of the C-terminal helix, forming hydrogen bonds with Asp-159^{HR1b} and Lys-161^{HR1b}.

Other residues in the core G protein domain that interact with HR1b include Lys-5^{Rac1} in the N-terminal β-strand and

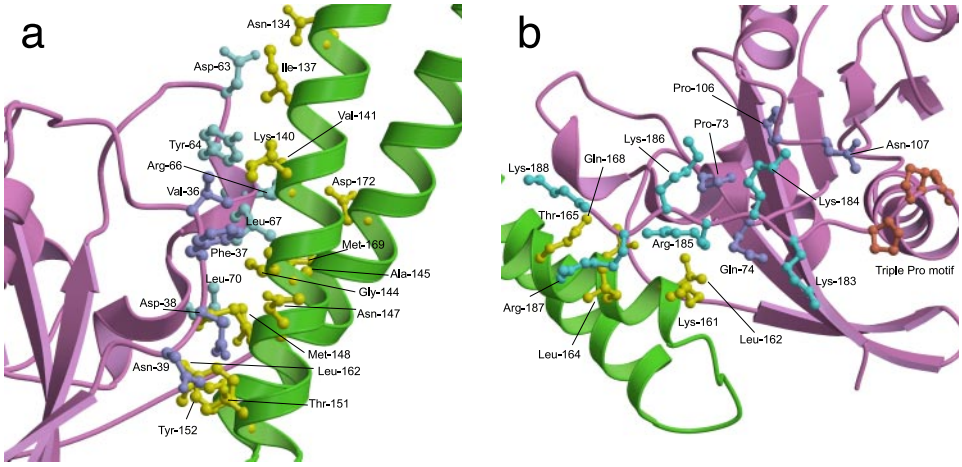

FIGURE 2. **Details of the interfaces between Rac1 and HR1b, with side chains shown in a ball-and-stick representation.** *a*, contacts involving residues in the switch regions of Rac1. Switch I side chains are colored *purple*, and switch 2 side chains are colored *cyan*. The HR1b residues within 4 Å of Rac1 are colored *yellow*. *b*, contacts involving residues at the C terminus of Rac1. The side chains of the triple Pro motif at the end of the final Rac1 α-helix are colored *orange*, the side chains in the C-terminal extension of Rac1 are colored *cyan*, and all other Rac1 side chains are *purple*. The HR1b residues within 4 Å of the Rac1 C terminus are shown in *yellow*.

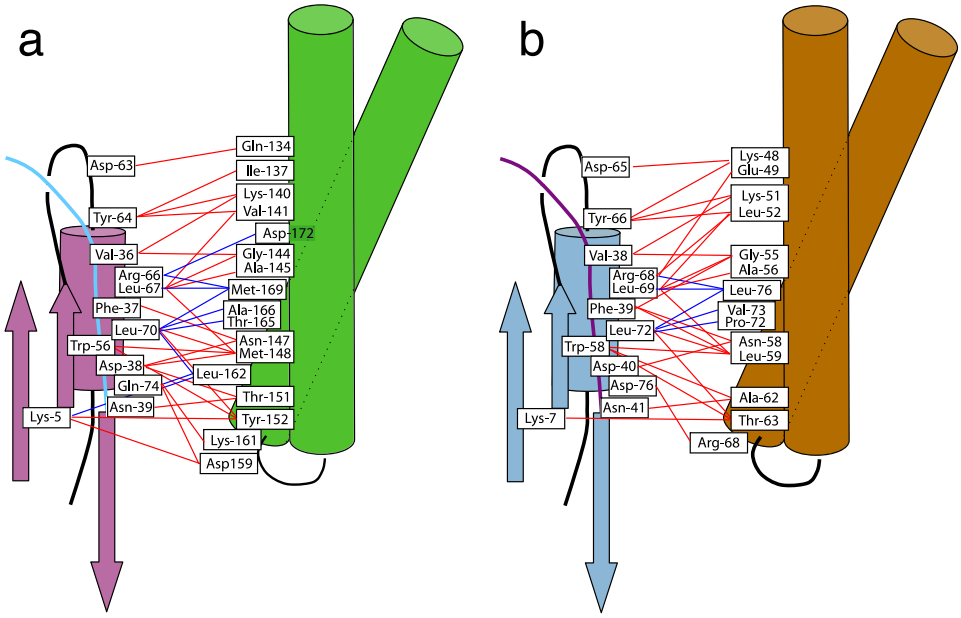

FIGURE 3. **Summary of Rac-HR1b and Rho-HR1a interactions with switch 1 and switch 2.** *a*, Rac1 with HR1b. The β-sheet at the N terminus of Rac1 and the switch 2 helix are colored *dark pink*, switch 1 is *blue*, and other loops are colored *black*. The HR1b helices are colored *green*. Contacts observed in the structures are shown as *lines* between the interacting residues and are colored *red* for interactions involving the N-terminal α-helix of HR1b and *blue* for interactions involving the C-terminal α-helix of HR1b. *b*, RhoA with HR1a (contact 2). The β-sheet at the N terminus of RhoA and the switch 2 helix are colored *pale blue*, switch 1 is *purple*, and other loops are colored black. The HR1a helices are colored *brown*. Contacts observed in the structures are shown as *lines* between the interacting residues and are colored *red* for interactions involving the N-terminal α-helix of HR1a and *blue* for interactions involving the C-terminal α-helix of HR1a.

Trp-56^{Rac1}, which is in the inter-switch region. These 2 residues are adjacent in the β-sheet and form a contact surface for residues in and around the hairpin loop of HR1b. Lys-5^{Rac1} makes hydrophobic contacts with Tyr-162^{HR1b}, Lys-158^{HR1b}, and Leu-162^{HR1b}, whereas its amino group is close to Asp-159^{HR1b}, forming a salt bridge in the structure (Fig. 3*A*). Trp-56^{Rac1} packs against the hydrophobic regions of the side chains of Met-148^{HR1b} and Tyr-152^{HR1b}.

The interactions with switch 1, also known as the effector loop because it is often involved in effector binding, are far less extensive and only involve residues in the N-terminal helix of the HR1b coiled-coil. Val-36^{Rac1} contacts the hydrophobic portion of the Lys-140^{HR1b} side chain and is also packed against Gly-144^{HR1b}. Asp-38^{Rac1} forms hydrogen bonds with Asn-147^{HR1b}, which also contacts Phe-37^{Rac1} and Thr-151^{HR1b}, which also contacts Asn-39^{Rac1} (Figs. 2*A* and 3*A*).

Interactions with the C Terminus—Unusually for a structural study, the Rac1 construct used in this investigation included the C terminus, which encompasses the PBR, whose structure is far less well characterized than that of the core domain. The final α-helix of the core domain finishes at Cys-178^{Rac1}, and this is immediately followed by 3 Pro residues. The triple Pro motif is unique to Rac1 among the Ras superfamily, although several small G proteins have 1 or 2 Pro residues in this region. The presence of 3 Pro residues fixes the position of the protein backbone into a polyproline helix (Fig. 2*b*). Furthermore, the presence of the PBR, which has 6 basic residues, forces the backbone to be extended to prevent charge clashes, which would be unavoidable in a more compact structure. Thus, overall, the juxtaposition of the triple Pro motif and the PBR fixes the conformation of the C terminus from the end of the final α-helix to Lys-188, which is the final residue before the site of lipid modification. The consequence of this is that the C-terminal residues loop back and interact with residues in the core G protein domain (Fig. 2*b*). Interestingly, residues in the C-terminal PBR also interact with HR1b. The main contacts with the core G protein domain are between Lys-183 ^{Rac1}, Lys-184 ^{Rac1}, and Arg-185 ^{Rac1} at the beginning of the PBR and Pro-73 ^{Rac1} and Gln-74^{Rac1} at the end of switch 2 and Cys-105 ^{Rac1}, Pro-106 ^{Rac1}, and Asn-107 ^{Rac1} in the loop between helix 3 and strand 5 (Fig. 2*b*). Arg-185 ^{Rac1} also forms hydrogen bonds with Thr-165^{HR1b} and Gln-168^{HR1b} and contacts Lys-161^{HR1b} and Leu-162^{HR1b}. Lys-186^{Rac1} makes few contacts with either HR1b or the core G protein domain. The methylenes of Arg-187^{Rac1} contact the side chain of Leu-164^{HR1b}, whereas the Lys-188^{Rac1} side chain contacts Gln-168^{HR1b} and Leu-164^{HR1b}.

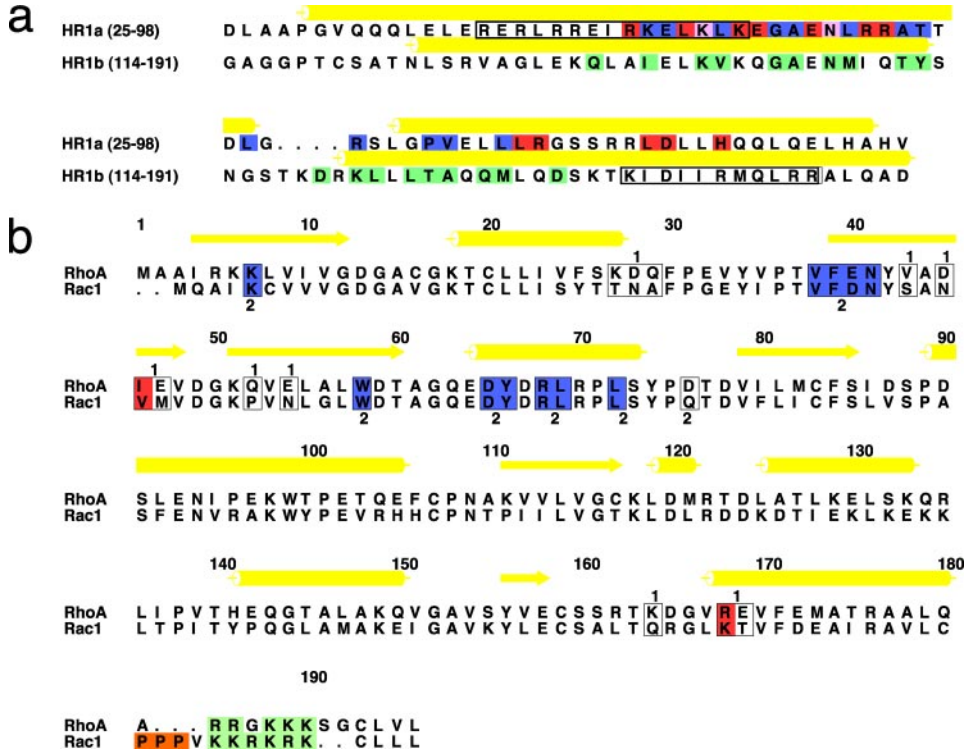

FIGURE 4. **Sequence alignments.** Secondary structures are indicated in *yellow* above each alignment; helices are shown as *cylinders*, and strands as shown as *arrows*. *a*, alignments of HR1 domains from PRK. Residues in HR1a that interact with RhoA in contact 1 are shaded *red*, those in contact 2 are shaded *blue*, and those in both contact 1 and contact 2 are shaded *pink*. Residues in HR1b that interact with Rac1 are shaded *green*. The pseudosubstrate site in HR1a and a potential pseudosubstrate site in HR1b are *boxed*. *b*, alignments of Rac1 and RhoA. Residues in RhoA that interact with HR1a in contact 1 and contact 2 are *boxed* and are shaded *red* (contact 1) or *blue* (contact 2) if they are conserved. The triple proline motif in Rac1 is shaded in *orange*, and the PBR is shaded in *green*.

It is apparent that the contacts made between HR1b and the Rac1 C terminus are not extensively ionic. Rather, the driving force for the interaction seems to be a combination of the triple Pro motif causing the conformation of the backbone to be fixed, the interactions with residues in the core G protein domain and the requirement for the PBR itself to be extended, which decreases the repulsion between the adjacent basic side chains.

The interactions of G proteins with their effectors generally require the G protein to be active, *i.e.* GTP-bound. HR1b interacts with both switch 1 and switch 2 of Rac1 (Fig. 4*a*), and the binding affinity for these regions is likely to be nucleotide-dependent. The C terminus of Rac1 is not directly in contact with the bound nucleotide, so it is less obvious whether the affinity for this region will be nucleotide-dependent. The C-terminal region does, however, interact with Pro-73 and Gln-74, which are adjacent to switch 2 in the sequence. These residues could be sensitive to the conformation of switch 2, which in turn is sensitive to the bound nucleotide, leading to nucleotide dependence for the PBR as well. The size of the interaction surface between HR1b and Rac1 that involves the switches is ~1,500 Å^2 and should therefore be sufficient to confer nucleotide dependence.

Implications for Membrane Attachment—The basic sequences at the C termini of small G proteins are thought to be important for membrane attachment. The GDP-bound Rho family members are sequestered within the cell by interactions with GDI proteins, but activation of the Rho protein leads to the exchange of GDP for GTP and membrane localization. The interaction of a PBR at the C terminus with the negative head groups of phospholipids stabilizes the membrane localization of G proteins that have only one lipid modification (reviewed in Ref. 24).

The nature of the interactions with HR1b means that the methylene portions of at least some of the Lys and Arg side chains in the PBR are buried, leaving the charged moieties at the end of the side chains solvent-exposed. Several residues of the PBR are, therefore, still available to interact with the membrane (Fig. 5). Interestingly, HR1b is also relatively basic, and in the complex with Rac1, Lys-161 is also close to the membrane and could potentially enhance the interaction with the membrane phospholipid head groups. The C terminus of Rac1 is less well defined in the structure than the G domain core, and it is also possible that the interactions between the PBR and the membrane consolidate the position of the PBR with respect to the rest of the G protein, conferring a concomitant increase in the affinity for PRK1.

Effects of Rac1 Mutations—Several of the Rac1 residues that interact with HR1b in the structure abrogate the interaction when they are mutated to Ala (22). The interactions involving switch 2 are predominantly hydrophobic and include Asp-63, Arg-66, Tyr-64, Leu-67, Leu-70, and Gln-74. Mutation of Leu-67, Leu-70, and Tyr-64 have relatively modest effects on the affinity, decreasing it 2–6-fold. This is presumably because introduction of the smaller Ala side chain, which is still hydrophobic, can be accommodated by a slight rearrangement of the flexible switches. Mutation of Asp-63 to Ala, in contrast, decreased the affinity more than 15-fold, suggesting that introduction of an uncharged residue at this position cannot be tolerated. Surprisingly, mutations of residues in Rac1 that are relatively distant from the binding site of HR1b can also abrogate binding. These residues include Ala-27 and Gln-162, which pack behind switch 1, Lys-166, and Thr-167 in the C-terminal α-helix and Asn-43, which is in the three-stranded β-sheet. We have found in previous work with small G proteins that residues that do not directly contact the effector, but are in the regions that pack behind the effector-binding regions, can be thermodynamically important for interactions (41). It is likely therefore that mutation of these residues causes subtle rearrangements in the molecular topography of the binding surface that prevent tight binding of the effector.

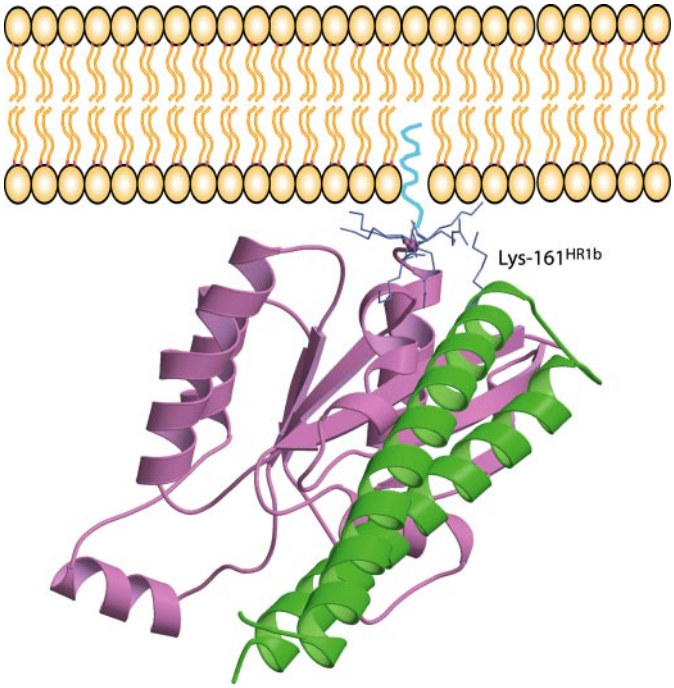

FIGURE 5. **Interaction with HR1b would not prevent the PBR contacting the plasma membrane.** Several of the basic residues (colored *blue*) in the C terminus of Rac1 are still free to form electrostatic contacts with the negatively charged phospholipid head groups and enhance binding to the membrane.

Mutations in the C-terminal PBR of Rac1 also abrogate binding to HR1b by more than 15-fold. In this case, mutation of any of the basic residues to Ser has a severe effect on binding. The effects of these mutations are likely to be structural; removal of a positive charge decreases the repulsion between the side chains and relaxes the constraints that force the C terminus to be extended. When the PBR is no longer extended, the favorable interactions with HR1b are lost, and the affinity drops dramatically.

Comparison with Other Rac Effector Complexes—There are a number of Rac1-effector complexes whose structures have been solved to date. In all these complexes, the Rac1 used was truncated at the C terminus. Although it cannot be precluded that the C terminus would participate in some of these effector complexes if it were included, high affinity binding can be achieved with the truncated protein, suggesting that the C terminus is not thermodynamically important for the interaction with these effectors. The Rac-binding region from $p67^{phox}$ is also α-helical and forms a series of coiled-coils, but it does not contact switch 2; rather, it makes most of its contacts with switch 1 (42). The pleckstrin homology domain in the recently solved phospholipase Cβ2-Rac complex does contact switch 2 but does not use an α-helix to contact the switch 2 helix in a coiled-coil arrangement (43). Instead, switch 2 binds to a β-strand and the C-terminal end of the pleckstrin homology domain α-helix. There is one effector of Rac1 that forms a coiled-coil interaction with switch 2; Arfaptin 2 is a crescent-shaped dimer, where each monomer comprises a three-helix bundle (44). Two of the helices in the coiled-coil interact with the Rac1, in a similar way to that in which HR1b interacts with Rac1. The relative orientations of the helices, however, are different; in Rac1-HR1b, the N-terminal HR1b helix is parallel to the switch 2 helix, whereas in Rac1-Arfaptin 2, the N-terminal Arfaptin 2 helix is anti-parallel to the switch 2 helix. The plasticity of helical interactions with switch 2 has been discussed previously in the context of the Arl1-GRIP domain complex structure (45). Essentially, the interfaces with the switch 2 helix are usually principally hydrophobic in nature and thus are non-directional, so there are no restraints on the orientation of the helices.

Comparison with the Structure of HR1a-RhoA—The structure of the first HR1 repeat of PRK1 (HR1a) in complex with RhoA has been solved and showed that although the stoichiometry of the complex in the crystals was 1:1, there were two potential contact sites between RhoA and HR1a (46). The major contact site (contact 1) is very different from the HR1b-Rac1 complex and involves interactions with helix 1, the inter-switch anti-parallel β-sheet, and the C-terminal α-helix. Contact 2, on the other hand, involves interactions with switch 1 and switch 2 that are strikingly similar to the HR1b-Rac1 complex. From a comparison of the HR1a-RhoA interactions in contact 2 with those in the HR1b-Rac1 complex (Fig. 3), it is clear that the pattern of hydrophobic and hydrogen bond interactions is similar in the two complexes.

The switch residues of Rac1 and RhoA that interact with HR1b and HR1a (contact 2), respectively, either are identical or have conservative substitutions (Figs. 3 and 4B). It might therefore be expected that HR1b could bind to both Rac1 and RhoA. The C-terminal region of RhoA, however, is not the same as the Rac1 C terminus (Fig. 3*B*). It has only a single Pro residue, and a Gly residue interrupts the basic stretch of amino acids. As discussed, these changes are likely to lead to a different structure for the C-terminal region of RhoA, which renders it incompetent for HR1b binding. This leads to a decrease in affinity of at least 15-fold when HR1b binds to RhoA rather than Rac1 (22).

The Rac1-HR1b interaction buries 2,180 Å^2, whereas the RhoA-HR1a contact 2 interface buries 1,640 Å^2. If the Rac1 C-terminal interactions are removed, the buried surface area of the remaining Rac1-HR1b interface is 1,550 Å^2, similar to that of contact 2 RhoA-HR1a. The increased affinity of HR1b for Rac1 is thus likely to be due to the C-terminal interactions. This is supported by mutagenesis data that showed that mutations in the PBR change the affinity of Rac1 for HR1b to a similar level to that of RhoA for HR1b (22).

The residues in the HR1 domains that interact with the switch regions of Rac1 and RhoA (contact 2) are not as well conserved (Figs. 3 and 4A), particularly in the second α-helix of the coiled-coil. Thus, although they interact with conserved residues in the G proteins, there are several small differences in the detailed interactions (Fig. 3), and it is likely therefore that there will be subtle differences in the thermodynamics of the two interfaces.

Modeling RhoA and Rac1 Interactions with PRK1—PRK1 contains three HR1 domains, but all of the structural information available pertains only to isolated HR1a and HR1b in complex with G proteins. So how do HR1a and HR1b bind to the Rho family proteins in the context of full-length PRK1, and how does this relate to regulation of the kinase *in vivo*? We and others have shown that HR1a binds to RhoA much more tightly

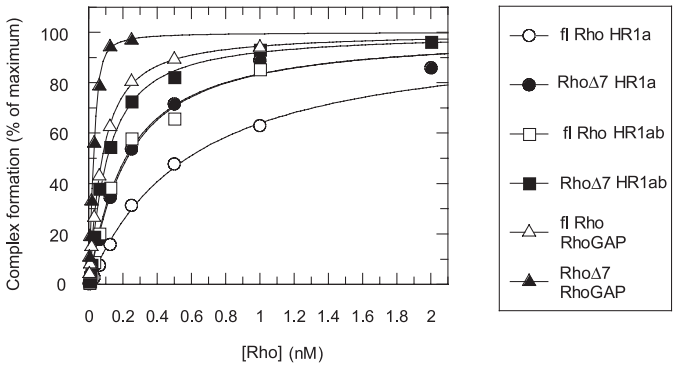

FIGURE 6. **Measurement of the affinity of RhoA Q63L·GTP for GST-HR1a, GST-HR1ab, or GST-RhoGAP.** The indicated concentrations of RhoA Q63L·GTP were incubated with 30 nM GST effector protein in SPAs. The SPA signal was corrected by subtraction of a blank in which the GST effector was omitted from the assay. The effect of the [RhoA] on the corrected SPA counts/min was fitted to a binding isotherm to give the apparent K_d value and the maximum signal at saturating concentrations of RhoA. The data are expressed as a percentage of the maximum signal. *FL*, full-length.

TABLE 2

Affinities of full-length and truncated RhoA for HR1a and HR1ab

Equilibrium binding constants were determined by SPA. K_d values are quoted with the standard errors from curve fitting.

	Apparent K_d		
	HR1a	HR1ab	RhoGAP
		nM	
fl-RhoA·GTP	538.8 ± 76.7	189.4 ± 32.1	55.7 ± 1.6
Δ7RhoA·GTP	187.6 ± 7.4	82.6 ± 7.1	5.6 ± 1.9

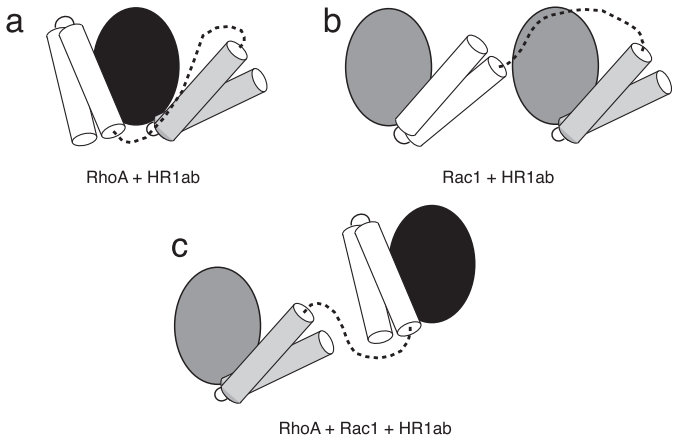

FIGURE 7. **Potential modes of interaction of HR1ab with RhoA and Rac1, based on the available structures and binding data.** HR1a is depicted as *white cylinders*, HR1b as *gray cylinders*, RhoA as a *black oval*, and Rac1 as a *gray oval*. *a*, from the x-ray structure, HR1a binds RhoA via contact 1, which involves residues in the C-terminal α-helix. Although free HR1b does not have a high affinity for RhoA, it would be in a position to engage with residues in contact 2. *b*, our data show that HR1a and HR1b can both bind Rac1, raising the possibility that two Rac1 molecules can bind to PRK1. *c*, since RhoA and Rac1 can both engage HR1a and HR1b domains, it is likely that the G proteins could bind to PRK1 simultaneously. This may only occur *in vitro* since RhoA and Rac1 are likely to be localized in different subcompartments in the cell.

than HR1b binds to RhoA (22, 23). The HR1b-Rac1 and HR1a-RhoA contact 2 interfaces are similar and, as discussed, many of the residues involved are conserved. We have measured the affinities of full-length RhoA and truncated (Δ7) RhoA for both HR1a and HR1ab by scintillation proximity assays (Fig. 6 and Table 2). The K_d values for HR1a and HR1ab binding to Δ7 RhoA and full-length RhoA are very similar; indeed, the Δ7 binds with a 2–3-fold higher affinity, probably because the Δ7 protein is more stable. In contrast, we found previously that HR1a, HR1b, and HR1ab all bind to Δ7 Rac1 with more than 10-fold lower affinity than to fl Rac1 (22). As Rac1 uses the C-terminal PBR for contacting HR1 repeats and RhoA does not, it is not possible to predict which is the true contact site between RhoA and HR1a. Nevertheless, contact 1 has a higher buried surface in the HR1a-RhoA structure, so it could be a high affinity binding site. That HR1a binds to RhoA through contact 1 is in agreement with data that show that HR1a binds to GDP·RhoA with only 4-fold lower affinity than to GTP-RhoA (23) since the RhoA residues in the contact 1 interface are likely to be less sensitive to the bound nucleotide than the contact 2 residues. Once HR1a is bound to contact 1, it is possible that HR1b could bind at the contact 2 site of RhoA as shown in the model in Fig. 7. The binding of HR1b to RhoA, although having a low affinity in isolation, would be enhanced by the presence of the high affinity binding of HR1a to RhoA at contact 1 and is consistent with the ~2-fold increase in the affinity of HR1ab for RhoA when compared with HR1a alone (22). The linker region between HR1a and HR1b in PRK1 is 26 residues long, which is sufficient to allow such an orientation of the two domains.

Rac1, conversely, binds to both HR1a and HR1b with a high affinity, and the affinity of HR1ab is the same as the HR1b affinity. Furthermore, the binding of HR1a, HR1b, and HR1ab to Rac1 required an intact C-terminal PBR (22). It is more likely, therefore, that HR1a and HR1b compete for binding to Rac1 and that both domains bind to the interface described in this work, which includes the C-terminal PBR. This suggests that two Rac molecules can bind simultaneously to PRK1 (Fig. 7). The linker between the HR1 domains is at least 20 amino acids long and includes multiple Gly and Pro residues. The long flexible linker between the HR1 domains would allow the HR1a and HR1b domains to interact independently with multiple G proteins.

The presence of two independent G protein binding domains in a single protein connected by a long flexible linker also raises the intriguing possibility that PRK1 could simultaneously bind to both Rac1 and RhoA. Our data suggest that such an interaction would involve HR1a binding to RhoA via contact 1 and HR1b binding to Rac1 via contact 2 (Fig. 7). This interaction may only be possible *in vitro* since it is not clear whether Rac1 and RhoA can localize to the same membrane subcompartment in the cell.

The HR1a domain is postulated to include an autoinhibitory sequence (5), but it has also been shown that removal of this domain alone is not sufficient for full kinase activation (47). Inspection of the sequence of HR1b reveals two potential pseudosubstrate sites (Fig. 4*a*), indicating that Rac binding to HR1b may also be functionally important with regards to activation. Despite the fact that several small G protein effectors are common to more than one GTPase, to our knowledge, no other effector has the ability to be simultaneously activated by more than one G protein.

Rac1 and RhoA binding to the HR1 domains could also be important for targeting of PRK1. As mentioned, above, Rac1 and RhoA may be present in different cellular subcompartments, *e.g.* in a migrating cell, Rac1 is present in lamellipodia at

the leading edge, whereas RhoA is located in the uropod (reviewed in Ref. 48). Their interaction with PRK1 would allow the kinase to be activated at different locations in the cell. Furthermore, the observation that RhoA only binds strongly to the HR1a domain, whereas Rac1 can engage both domains, implies that the two G proteins may lead to difference levels of kinase activity. The *in vivo* effects of multiple binding to G proteins may be the key that unlocks the mystery of the activation mechanism of this important kinase. The solution to this conundrum must await structural information involving multiple PRK1 HR1 domains and Rho family small GTPases.

REFERENCES

1. Takai, Y., Sasaki, T., and Matozaki, T. (2001) *Physiol. Rev.* **81,** 153–208
2. Zhao, Z. S., and Manser, E. (2005) *Biochem. J.* **386,** 201–214
3. Mukai, H. (2003) *J. Biochem.* **133,** 17–27
4. Watanabe, G., Saito, Y., Madaule, P., Ishizaki, T., Fujisawa, K., Morii, N., Mukai, H., Ono, Y., Kakizuka, A., and Narumiya, S. (1996) *Science* **271,** 645–648
5. Kitagawa, M., Shibata, H., Toshimori, M., Mukai, H., and Ono, Y. (1996) *Biochem. Biophys. Res. Commun.* **220,** 963–968
6. Vincent, S., and Settleman, J. (1997) *Mol. Cell. Biol.* **17,** 2247–2256
7. Lu, Y., and Settleman, J. (1999) *Genes Dev.* **13,** 1168–1180
8. Takahashi, M., Mukai, H., Toshimori, M., Mlyamoto, M., and Ono, Y. (1998) *Proc. Natl. Acad. Sci. U. S. A.* **95,** 11566–11571
9. Matsuzawa, K., Kosako, H., Inagaki, N., Shibata, H., Mukai, H., Ono, Y., Amano, M., Kaibuchi, K., Matsuura, Y., Azuma, I., and Inagaki, M. (1997) *Biochem. Biophys. Res. Commun.* **234,** 621–625
10. Kawamata, T., Taniguchi, T., Mukai, H., Kitagawa, M., Hashimoto, T., Maeda, K., Ono, Y., and Tanaka, C. (1998) *J. Neurosci.* **18,** 7402–7410
11. Taniguchi, T., Kawamata, T., Mukai, H., Hasegawa, H., Isagawa, T., Yasuda, M., Hashimoto, T., Terashima, A., Nakai, M., Ono, Y., and Tanaka, C. (2001) *J. Biol. Chem.* **276,** 10025–10031
12. Metzger, E., Muller, J. M., Ferrari, S., Buettner, R., and Schule, R. (2003) *EMBO J.* **22,** 270–280
13. Gao, Q. S., Kumar, A., Srinivasan, S., Singh, L., Mukai, H., Ono, Y., Wazer, D. E., and Band, V. (2000) *J. Biol. Chem.* **275,** 14824–14830
14. Misaki, K., Mukai, H., Yoshinaga, C., Oishi, K., Isagawa, T., Takahashi, M., Ohsumi, K., Kishimoto, T., and Ono, Y. (2001) *Proc. Natl. Acad. Sci. U. S. A.* **98,** 125–129
15. Shibata, H., Oda, H., Mukai, H., Oishi, K., Misaki, K., Ohkubo, H., and Ono, Y. (1999) *Mol. Brain Res.* **74,** 126–134
16. Morissette, M. R., Sah, V. P., Glembotski, C. C., and Brown, J. H. (2000) *Am. J. Physiol.* **278,** H1769–H1774
17. Cottone, G., Baldi, A., Palescandolo, E., Manente, L., Penta, R., Paggi, M. G., and De Luca, A. (2006) *J. Cell. Physiol.* **207,** 232–237
18. Balendran, A., Casamayor, A., Deak, M., Paterson, A., Gaffney, P., Currie, R., Downes, C. P., and Alessi, D. R. (1999) *Curr. Biol.* **9,** 393–404
19. Flynn, P., Mellor, H., Casamassima, A., and Parker, P. J. (2000) *J. Biol. Chem.* **275,** 11064–11070
20. Dong, L. Q., Landa, L. R., Wick, M. J., Zhu, L., Mukai, H., Ono, Y., and Liu, F. (2000) *Proc. Natl. Acad. Sci. U. S. A.* **97,** 5089–5094
21. Flynn, P., Mellor, H., Palmer, R., Panayotou, G., and Parker, P. J. (1998) *J. Biol. Chem.* **273,** 2698–2705
22. Owen, D., Lowe, P. N., Nietlispach, D., Brosnan, C. E., Chirgadze, D. Y., Parker, P. J., Blundell, T. L., and Mott, H. R. (2003) *J. Biol. Chem.* **278,** 50578–50587
23. Blumenstein, L., and Ahmadian, M. R. (2004) *J. Biol. Chem.* **279,** 53419–53426
24. Williams, C. L. (2003) *Cell. Signal.* **15,** 1071–1080
25. ten Klooster, J. P., Jaffer, Z. M., Chernoff, J., and Hordijk, P. L. (2006) *J. Cell Biol.* **172,** 759–769
26. Thompson, G., Owen, D., Chalk, P. A., and Lowe, P. N. (1998) *Biochemistry* **37,** 7885–7891
27. Ferentz, A. E., and Wagner, G. (2000) *Q. Rev. Biophys.* **33,** 29–65
28. Nietlispach, D., Ito, Y., and Laue, E. D. (2002) *J. Am. Chem. Soc.* **124,** 11199–11207
29. Zwahlen, C., Legault, P., Vincent, S. J. F., Greenblatt, J., Konrat, R., and Kay, L. E. (1997) *J. Am. Chem. Soc.* **119,** 6711–6721
30. Salzmann, M., Pervushin, K., Wider, G., Senn, H., and Wuthrich, K. (1998) *Proc. Natl. Acad. Sci. U. S. A.* **95,** 13585–13590
31. Salzmann, M., Wider, G., Pervushin, K., Senn, H., and Wuthrich, K. (1999) *J. Am. Chem. Soc.* **121,** 844–848
32. Merritt, E. A., and Bacon, D. J. (1997) *Methods Enzymol.* **277,** 505–524
33. Kraulis, P. J., Domaille, P. J., Campbell-Burk, S. L., Van Aken, T., and Laue, E. D. (1994) *Biochemistry* **33,** 3515–3531
34. Cornilescu, G., Delaglio, F., and Bax, A. (1999) *J. Biomol. NMR* **13,** 289–302
35. Brunger, A. T., Adams, P. D., Clore, G. M., DeLano, W. L., Gros, P., Grosse-Kunstleve, R. W., Jiang, J. S., Kuszewski, J., Nilges, M., Pannu, N. S., Read, R. J., Rice, L. M., Simonson, T., and Warren, G. L. (1998) *Acta Crystallogr. Sect. D Biol. Crystallogr.* **54,** 905–921
36. Linge, J. P., O'Donoghue, S. I., and Nilges, M. (2001) *Methods Enzymol.* **339,** 71–90
37. Graham, D. L., Eccleston, J. F., and Lowe, P. N. (1999) *Biochemistry* **38,** 985–991
38. Ito, Y., Yamasaki, K., Iwahara, J., Terada, T., Kamiya, A., Shirouzu, M., Muto, Y., Kawai, G., Yokoyama, S., Laue, E. D., Walchli, M., Shibata, T., Nishimura, S., and Miyazawa, T. (1997) *Biochemistry* **36,** 9109–9119
39. Feltham, J. L., Dotsch, V., Raza, S., Manor, D., Cerione, R. A., Sutcliffe, M. J., Wagner, G., and Oswald, R. E. (1997) *Biochemistry* **36,** 8755–8766
40. Hirshberg, M., Stockley, R. W., Dodson, G., and Webb, M. R. (1997) *Nat. Struct. Biol.* **4,** 147–152
41. Elliot-Smith, A. E., Mott, H. R., Lowe, P. N., Laue, E. D., and Owen, D. (2005) *Biochemistry* **44,** 12373–12383
42. Lapouge, K., Smith, S. J. M., Walker, P. A., Gamblin, S. J., Smerdon, S. J., and Rittinger, K. (2000) *Mol. Cell.* **6,** 899–907
43. Jezyk, M. R., Snyder, J. T., Gershberg, S., Worthylake, D. K., Harden, T. K., and Sondek, J. (2006) *Nat. Struct. Mol. Biol.* **13,** 1135–1140
44. Tarricone, C., Xiao, B., Justin, N., Walker, P. A., Rittinger, K., Gamblin, S. J., and Smerdon, S. J. (2001) *Nature* **411,** 215–219
45. Panic, B., Perisic, O., Veprintsev, D. B., Williams, R. L., and Munro, S. (2003) *Mol. Cell* **12,** 863–874
46. Maesaki, R., Ihara, K., Shimizu, T., Kuroda, S., Kaibuchi, K., and Hakoshima, T. (1999) *Mol. Cell.* **4,** 793–803
47. Yoshinaga, C., Mukai, H., Toshimori, M., Miyamoto, M., and Ono, Y. (1999) *J. Biochem.* (*Tokyo*) **126,** 475–484
48. Jaffe, A. B., and Hall, A. (2005) *Annu. Rev. Cell Dev. Biol.* **21,** 247–269
49. Kraulis, P. J. (1991) *J. Appl. Crystallogr.* **24,** 946–950

The Rac1 Polybasic Region Is Required for Interaction with Its Effector PRK1

Rakhee Modha, Louise J. Campbell, Daniel Nietlispach, Heeran R. Buhecha, Darerca Owen and Helen R. Mott

J. Biol. Chem. 2008, 283:1492-1500.
doi: 10.1074/jbc.M706760200 originally published online November 15, 2007
